Journal of Solid State Chemistry **168,** 396–407 (2002)
doi:10.1006/jssc.2002.9687

Structural and Physical Properties of New Conducting Cation Radical Salts with Te-Based Counteranions, Tetraiodotellurate(II) and Hexaiododitellurate(II)

Masahiro Fujiwara,* Naoya Tajima,† Tatsuro Imakubo,† Masafumi Tamura,† and Reizo Kato†,[1]

*The Institute for Solid State Physics, The University of Tokyo, 5-1-5 Kashiwanoha, Kashiwa-shi, Chiba 277-8581, Japan; and †RIKEN (The Institute of Physical and Chemical Research), Hirosawa, 2-1 Wako-shi, Saitama 351-0198, Japan

Received December 15, 2001; in revised form April 4, 2002; accepted April 10, 2002

This article reports preparation, structure, and conducting property of several cation radical salts of organic donors tetramethyltetrathiafulvalene (TMTTF), ethylenedithiotetrathiafulvalene (EDT-TTF), bis(ethylenedithio)tetrathiafulvalene (ET), bis(ethylenedithio)tetraselenafulvalene (BETS) and hexamethylenetetraselenafulvalene (HMTSF) with two novel planar Te-based dianions, TeI_4^{2-} and $Te_2I_6^{2-}$. $(ET)_5Te_2I_6$ 1 and $(BETS)_5Te_2I_6$ 2 are isostructural. In these $Te_2I_6^{2-}$ salts, intermolecular short I···I contacts form a supramolecular corrugated anion sheet. Donor arrangement is similar to the θ-type. With lowering temperature, the resistivity of 1 shows a gradual increase followed by a sharp upturn at 110 K. 2 is metallic down to 120 K and shows a gradual increase of the resistivity followed by a clear transition to an insulating state around 60 K. Crystal structure of $(ET)_4TeI_4$ 3 is based on the "herring bone" arrangement of ET molecules similar to the α-type. 3 shows a semiconductive behavior around room temperature followed by a transition to an insulating state at 210 K. $(EDT\text{-}TTF)_4TeI_4$ 4, a semiconductor, exhibits a unique two-dimensional arrangement of dimerized EDT-TTF molecules. © 2002 Elsevier Science (USA)

Key Words: **molecular conductor; TTF derivatives; tellurium-halide anion; crystal structure; band structure; electric resistivity.**

INTRODUCTION

Chalcogen-rich organic donors, for example tetrathiafulvalene (TTF) derivatives, are known to form a wide range of cation radical salts, including semiconductors, metals, and superconductors, with inorganic anions (1). They exhibit a wide variety of crystal structures. Their physical properties are governed by arrangement, orientation and formal charge of component donor molecules. The closed-shell counter anions do not form a conduction band, but their size, shape, and charge often have significant influence on crystal structures and thus the physical properties of the cation radical salts. For instance, most known superconducting cation radical salts with high transition temperature contain polymeric anion networks which seem to be suitable for the formation of the so-called κ-type donor arrangement (2). For the control of the arrangement, orientation and formal charge of the donor molecule, much more attention should be paid to a survey of distinctive counter anions (2–4).

On the other hand, structural and bonding properties of chalcogen halides have been a fascinating subject of structural chemistry. The stereochemistry of the chalcogen halides exhibits a large range because of the strongly variable stereochemical activity of the inert electron pairs in the valence shell of the chalcogen atom (5). In the solid state, their structural nature cannot be readily predicted and described using simple valence shell electron pair repulsion (VSEPR) model. This is determined by secondary effects (6) such as maximization of Coulomb forces by ion formation and by association effects of various kinds. Nevertheless, we are able to predict that mono- or dinuclear halochalcogenates(II) have square planar geometry. Although inorganic anions with various shapes (including linear, tetrahedral, and octahedral ones) have been used as counterparts of cation radicals up to now, the number of square planar inorganic anions examined for the formation of molecular conductors are still limited (1).

With these points in mind, we synthesized and investigated planar tellurium-halide anions, TeI_4^{2-} and $Te_2I_6^{2-}$, as new counterparts of organic cation radicals. Five TTF derivatives: tetramethyltetrathiafulvalene (TMTTF), ethylenedithiotetrathiafulvalene (EDT-TTF), bis(ethylenedithio)tetrathiafulvalene (ET), bis(ethylenedithio)tetraselenafulvalene (BETS) and hexamethylenetetraselenafulvalene (HMTSF) were chosen as organic donors (Scheme 1). We

[1]To whom correspondence should be addressed. Fax: +81-48-462-4661. E-mail: reizo@postman.riken.go.jp.

0022-4596/02 $35.00

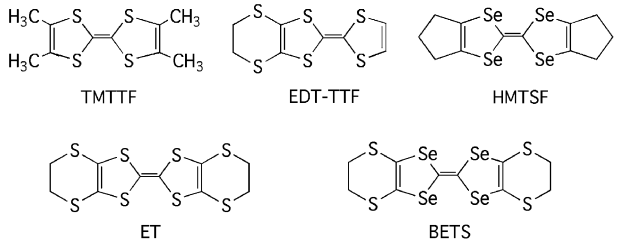

SCHEME 1

report here that they provide conducting cation radical salts with novel molecular arrangements. One of them, $Te_2I_6^{2-}$, has the ability to form a new type of supramolecular anion layer and can provide conducting cation radical salts with novel formal charge of the donor molecule.

EXPERIMENTAL

Synthesis and Preparation

All reagents were purchased and used as received. All synthetic reactions were carried out under Ar atmosphere. Donor molecules (7) and Me_2TeI_2 (8) were prepared by the literature method.

Synthesis of $Bu^n_4N \cdot TeI_3$

To 3.287 g (8.0 mmol) of Me_2TeI_2 dissolved in 80 mL $CHCl_3$, 2.975 g (8.0 mmol) of $Bu^n_4N \cdot I$ was added. After overnight stirring at room temperature, the reddish-brown reaction mixture turned dark and suspended with gray precipitate. The precipitate was removed by filtration and the residue was washed well with $CHCl_3$. Purple powder was isolated by concentration of the filtrate combined with the washings under reduced pressure. Recrystallization in $CHCl_3$ afforded purple plates (2.81 g, yield 45%).

Anal. calcd for $C_{16}H_{36}Te_1I_3$: C, 38.67; H, 7.30; N, 2.82. Found: C, 37.47; H, 7.26; N, 2.78.

Preparation of Cation Radical Salts

The cation radical salts based on the TTF derivatives were obtained by the galvanostatic electrolysis under Ar in the presence of $Bu^n_4N \cdot TeI_3$. An H-shaped 20 mL cell and Pt electrodes (1 mm diameter) were used. TeI_4^{2-} salts were obtained from a 1,2-dichloroethane or dichloromethane solution, while $Te_2I_6^{2-}$ salts were obtained from a chlorobenzene solution. Detailed conditions are given in Table 1.

Crystal Structure Determination

For all salts, intensity data were collected at room temperature on an automatic four-circle diffractometer (Rigaku AFC−7R) or a Weissenberg-type imaging plate (MAC science DIP320) with graphite-monochromated MoKα radiation. The ω–2θ scans were employed for data collection and Lorentz and polarization corrections were applied in the four-circle diffractometer measurements. An empirical absorption correction was carried out by azimuthal (psi-) scans of several reflections in the four-circle diffractometer measurements. In the case of the imaging plate, the absorption correction was included in the scaling process of the image data. For all the salts, lattice parameters were initially derived from more than 22 reflections measured by the four-circle diffractometer. Crystallographic data are listed in Table 2. The structures were solved by a direct method using SIR97 and refined by full-matrix least-squares method. Anisotropic thermal parameters were used for non-hydrogen atoms. All hydrogen atoms were added in calculated positions with fixed isotropic contributions. All calculations were performed with the use of "teXsan" crystallographic software package of Molecular Structure Co.

Resistivity Measurements

The d.c. resistivity measurements were performed with the standard four-probe method. Electrical contacts were obtained by gluing four gold wires (10 or 15 μm diameter) to the crystal with gold paste. Resistivity measurements under high pressure were performed using a clamp cell with the Daphne oil 7373 as the pressure medium. The pressure

TABLE 1
Conditions of Galvanostatic Electrochemical Crystallization

Formula	Donor (mg)	Electrolyte[a] (mg)	Current (μA)	Solvent[b] (20 mL)	Temperature (°C)	Period (days)	Appearance
$(BEDT\text{-}TTF)_5Te_2I_6$	15.4	54.3	0.2	CB	40	5	Black plate
$(BETS)_5Te_2I_6$	5.8	70.1	0.2	CB	40	14	Black plate
$(BEDT\text{-}TTF)_4TeI_4$	7.2	36.5	1.0	CH_2Cl_2	40	5	Black elongated plate
$(EDT\text{-}TTF)_4TeI_4$	13.4	84.2	0.5	CH_2Cl_2	5	20	Black plate
$(TMTTF)_2TeI_4$	11.6	57.6	0.2	CH_2Cl_2	20	3	Black rod
$(HMTSF)_2Te_2I_6$	3.5	36.5	0.2	CB	40	10	Black rod

[a] Electrolyte = $Bu^n_4N \cdot TeI_3$,
[b] CH_2Cl_2 could be replaced with 1,2-dichloroethane. CB = chlorobenzene.

TABLE 2
Crystal Data of Radical Cation Salts with Te-Based Planar Dianions

	$(ET)_5Te_2I_6$ **1**	$(BETS)_5Te_2I_6$ **2**	$(ET)_4TeI_4$ **3**	$(EDT\text{-}TTF)_4TeI_4$ **4**	$(TMTTF)_2TeI_4$ **5**	$(HMTSF)_2\ Te_2I_6$ **6**
Empirical formula	$C_{50}H_{40}I_6S_{40}Te_2$	$C_{50}H_{40}I_6S_{20}Se_{20}Te_2$	$C_{40}H_{32}I_4S_{32}Te$	$C_{32}H_{24}I_4S_{24}Te_1$	$C_{20}H_{24}I_4S_8Te_1$	$C_{24}H_{24}I_6Se_8Te_2$
Formula weight	2939.89	3877.89	2173.83	1813.20	1156.11	1960.76
Crystal system	*Monoclinic*	*Monoclinic*	*Triclinic*	*Orthorhombic*	*Monoclinic*	*Triclinic*
Space group	$P2_1/n$	$P2_1/n$	$P\bar{1}$	*Cmca*	$C2/m$	$P\bar{1}$
a (Å)	21.469(4)	21.637(1)	16.851(2)	29.584(9)	19.905(2)	10.284(6)
b (Å)	10.862(3)	10.760(4)	18.321(2)	12.438(4)	9.757(1)	12.767(7)
c (Å)	20.354(3)	21.001(7)	11.204(1)	14.387(7)	8.533(1)	8.421(7)
α (deg)	—	—	107.21(7)	—	—	99.31(5)
β (deg)	114.72(1)	115.72(3)	90.96(6)	—	101.926(5)	109.91(5)
γ (deg)	—	—	92.55(6)	—	—	70.21(4)
V (Å^3)	4311(1)	4405(3)	3299(2)	5293(3)	1621(1)	976(1)
Z	2	2	2	4	2	1
d_{calc} (g cm^{-3})	2.264	2.923	2.188	2.275	2.368	3.333
Refl. measured.	13 506	13 808	10 759	4171	1886	6027
Refl. independ.	12 568	8671	6767	2769	1886	6023
Refl. used ($I > 3\sigma$)	7391	5367	6767	2177	1464	2766
g.o.f.	1.16	2.21	3.23	2.22	1.10	1.96
Dimension (mm^3)	$0.51 \times 0.38 \times 0.04$	$0.82 \times 0.30 \times 0.02$	$0.30 \times 0.07 \times 0.05$	$0.89 \times 0.20 \times 0.02$	$0.50 \times 0.08 \times 0.02$	$0.85 \times 0.17 \times 0.02$
R, R_w	0.035, 0.051	0.061, 0.077	0.103, 0.133	0.048, 0.072	0.029, 0.038	0.079, 0.096
Diffractometer	4-circle	IP	IP	IP	IP	4-circle

at room temperature was calibrated with the NH_4F phase transition.

Band Calculation

For the estimation of intermolecular overlap integrals, highest occupied molecular orbital (HOMO) was obtained by the extended Hückel MO calculation (9). The calculation was carried out with the use of semiempirical parameters for Slater-type atomic orbital. The exponents ζ and ionization potentials (Ryd.) for atomic orbitals are listed in Table 3. It has been assumed that the transfer integral (t) is proportional to the overlap integral (S), $t = \varepsilon S$ ($\varepsilon = -10$ eV, ε is a constant with the order of the orbital energy of HOMO). The band structures were calculated based on the tight-binding approximation (10).

TABLE 3
The Exponents ζ and the Ionization Potentials I_p (Ryd.) for Atomic Orbitals

		ζ	$-I_p$ (Ryd.)
S	3*s*	2.122	1.620
	3*p*	1.827	0.770
Se	4*s*	2.112	1.471
	4*p*	1.827	0.809
C	2*s*	1.625	1.573
	2*p*	1.625	0.838
H	1*s*	1.00	1.00

RESULTS AND DISCUSSION

Synthesis and Structure of Counter Anions

The electrolyte $Bu^n_4N \cdot TeI_3$ was synthesized by a reaction of Me_2TeI_2 and $Bu^n_4N \cdot I$ in $CHCl_3$ with moderate yield. This method is more useful and simpler than the literature method (5) where the $Te_2I_6^{2-}$ anion was formed by the reaction of Te_4I_{16} (besides $Te_2I_{10}^{2-}$) with iodine in acetonitrile. $Bu^n_4N \cdot TeI_3$ is air stable in the solid state, but is quite unstable in tetrahydrofuran. The electrochemical crystallization using $Bu^n_4N \cdot TeI_3$ provided TeI_4^{2-} or $Te_2I_6^{2-}$ salt, strongly depending on the solvent. For each of these two anions, its geometry does not depend on the donor molecule. As typical examples, the crystal structures of these anions in ET salts are shown in Fig. 1. The dianion TeI_4^{2-} has a square planar shape with Te–I distances ranging from 2.89 to 3.02 Å that are almost the same as the literature value (2.985(2) Å (11)). The other dianion $Te_2I_6^{2-}$ consists of two edge-sharing distorted square of TeI_4 moiety. The bridging Te–I bond lengths (3.16 and 3.17 Å)

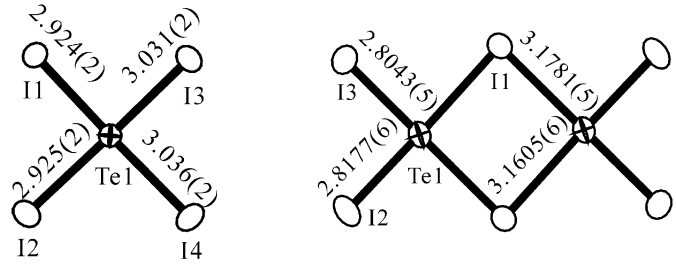

FIG. 1. Molecular structures of TeI_4^{2-} and $Te_2I_6^{2-}$ (in ET salts).

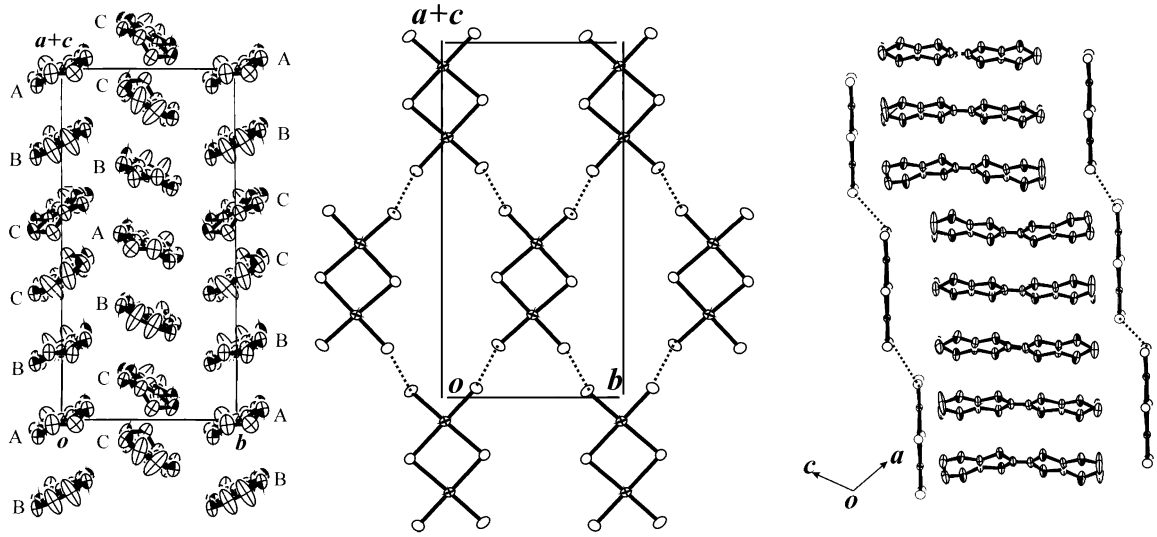

FIG. 2. Crystal structure of **1**: end-on projection of ET molecules (left), $Te_2I_6^{2-}$ anion network (middle) and side view (right).

are longer than the terminal Te–I bond lengths (2.80 and 2.81 Å).

*(ET)$_5$Te$_2$I$_6$ (**1**) and (BETS)$_5$Te$_2$I$_6$ (**2**)*

These isostructural 5:1 salts were obtained by galvanostatic electrolysis of solutions containing the corresponding donor molecule and $Bu^n_4N \cdot TeI_3$ in chlorobenzene. The crystal structure of **1** is shown in Fig. 2. **1** has a layered structure with a "herring-bone" donor arrangement. The unit cell contains two crystallographically equivalent ET stacks related by the two-fold screw axis along the ***b***-axis. The stack has a five-fold periodicity, ···CBABC···. In this sense, this structure can be described as a θ-type arrangement of the centrosymmetric ET pentamers. However, it should be noted that the formal charge of the ET unit ($+\frac{2}{5}$) is smaller than that of the conventional θ-type ET salts ($+\frac{1}{2}$), which leads to a difference in the band structure (vide infra). The array of donor molecules includes an almost parallel slip along the short molecular axis within the pentamer (Fig. 3) and a longitudinal shift between pentamers (Fig. 2). This longitudinal shift corresponds to the thickness of the anion. Short S···S, S···Se and Se···Se intermolecular contacts are observed between neighboring stacks but not within the same stack, which is normally observed in the conventional θ-type ET salts (Table 4, Fig. 3). The dihedral angles between the molecular planes of ET molecules in neighboring stacks (abbreviated as the dihedral angles) range from 120.2° to 127.5° in **1** and from 119.5° to 122.6° in **2**, respectively. For both salts, the bond length examination (12) suggests that the formal charge of donor molecules A and C is larger than that of B and there is no neutral donor molecule in the crystal.

In both salts, the anions are linked to each other through short intermolecular I···I contacts (3.67 Å) to form a supramolecular corrugated sheet. Fitting into this anion sheet, the donor layer exhibits a terrace-like structure, which is not observed in the conventional θ-type donor arrangement. In general, the donor molecules tend to exhibit the formal charge of $+\frac{1}{2}$ in conducting cation radical salts. In **1** and **2**, however, the donor molecules have an unusual (averaged) formal charge $+\frac{2}{5}$. The unit area of

TABLE 4
Short S···S, S···Se and Se···Se Intermolecular Contacts

Atom	Atom	Distance	Atom	Atom	Distance
(a) *In(ET)$_5$Te$_2$I$_6$ (**1**)*					
S(1)	S(17^a)	3.595(3)	S(7)	S(10^c)	3.580(3)
S(2)	S(18^b)	3.506(3)	S(8)	S(17^d)	3.569(3)
S(3)	S(20^c)	3.570(3)	S(9)	S(16^c)	3.454(2)
S(4)	S(18^b)	3.546(3)	S(9)	S(12^c)	3.583(3)
S(4)	S(19^d)	3.549(3)	S(10)	S(11^d)	3.570(2)
(b) *In(BETS)$_5$Te$_2$I$_6$ (**2**)*					
Se(1)	S(7^a)	3.448 (3)	Se(9)	S(4^d)	3.412(3)
Se(2)	S(8^b)	3.492(3)	Se(9)	S(2^d)	3.636(3)
Se(2)	Se(9^c)	3.699(2)	Se(10)	S(3^c)	3.455(3)
Se(3)	Se(10^d)	3.675(2)	Se(10)	S(1^c)	3.505(3)
Se(4)	Se(9^c)	3.550(2)	S(1)	S(7^a)	3.399(4)
Se(5)	S(8^d)	3.498(3)	S(1)	S(10^d)	3.454(4)
Se(5)	S(4^d)	3.544(3)	S(2)	S(9^c)	3.469(4)
Se(5)	Se(8^d)	3.675(2)	S(2)	S(8^b)	3.534(4)
Se(6)	S(3^c)	3.523(3)	S(3)	S(6^d)	3.515(4)
Se(6)	Se(7^c)	3.624(2)	S(3)	S(10^d)	3.560(4)
Se(6)	S(7^c)	3.623(3)	S(4)	S(5^c)	3.479(4)

$^a -\frac{1}{2}+x,\ \frac{1}{2}-y,\ -\frac{1}{2}+z.$
$^b -\frac{1}{2}+x,\ \frac{1}{2}-y,\ -\frac{1}{2}+z.$
$^c \frac{1}{2}-x,\ -\frac{1}{2}+y,\ \frac{1}{2}-z.$
$^d \frac{1}{2}-x,\ -\frac{1}{2}+y,\ \frac{1}{2}-z.$

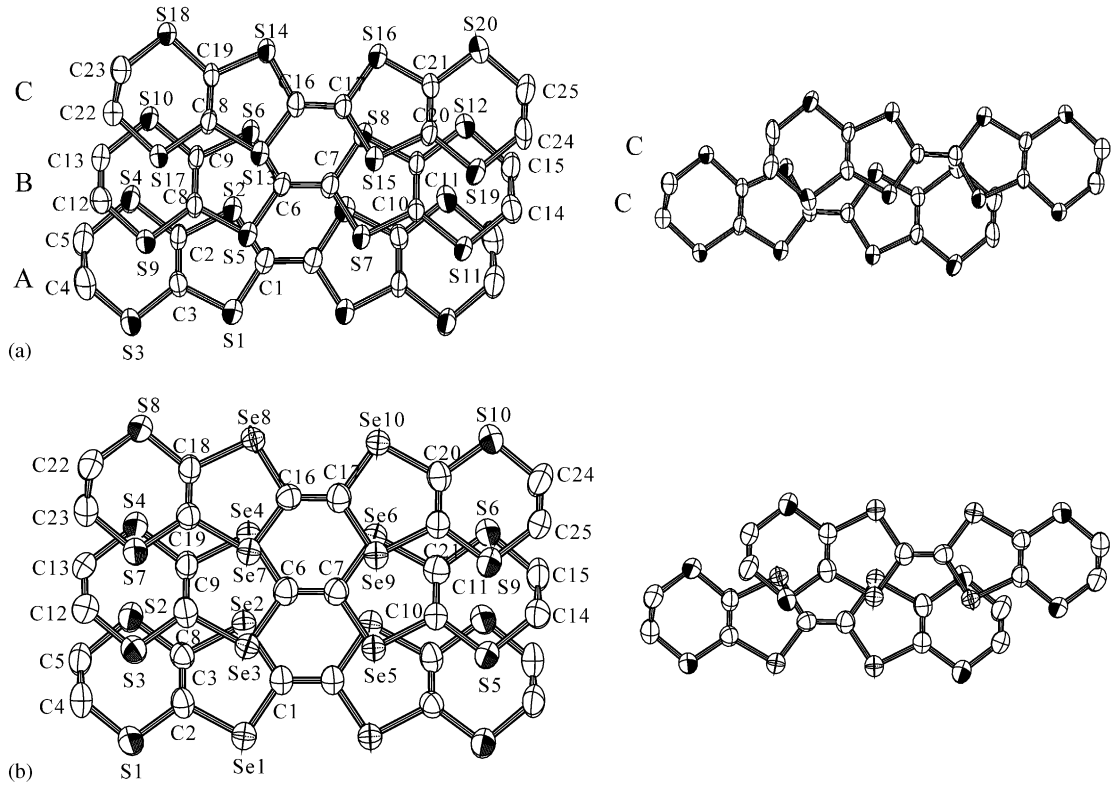

FIG. 3. Overlap modes of donor molecules: (a) intra-pentamer (left) and inter-pentamer (right) in **1**; (b) intra-pentamer (left) and inter-pentamer (right) in **2**.

the supramolecular anion layer has been reported to play an important role in the control of the donor/anion ratio and thus the formal charge (4). In rigid two-dimensional anion networks, the unit area of the layer can be defined more clearly than isolated discrete anion systems. The unit area of the anion network in **1** is 150 $Å^2$. One ET molecule is known to occupy 25–30 $Å^2$ in the conduction layer. To achieve compatibility between the anion part and the donor part, the ET molecules are obliged to form the unusual 5:1 salt (for the formation of the 4:1 salt corresponding the $+\frac{1}{2}$ formal charge, the unit area should be 100–120 $Å^2$). The unit area of the anion network possesses two electrons ($2e^-$) and thus the donor molecule has an averaged formal charge of $+\frac{2}{5}$. Since the $Te_2I_6^{2-}$ anions are connected with one another through the I···I contact, this supramolecular anion network is stiff. Indeed, the unit area of the anion layer in **2** does not change even for BETS with larger molecule size, which would be related to higher crystal density of **2** compared with those of conventional BETS salts (13).

The temperature dependence of the resistivity under pressure along the ***b***-axis for **1** and **2** is shown in Fig. 4. At ambient pressure, the resistivity of **2** shows a gradual increase followed by a sharp upturn at 110 K ($\rho_{r.t.} = 2\,\Omega$cm, $E_a = 0.05$ eV). Under pressure, a transition to an insulating state turns obscure and a shoulder appears around 160 K above 12 kbar. Unlike the conventional θ-type salts, the resistivity around room temperature monotonically decreases with pressure. At ambient pressure, the resistivity of **2** is low and almost independent of the temperature above about 100 K ($\rho_{r.t.} = 0.6\,\Omega$cm). Below 60 K, the resistivity remarkably increases as the temperature decreases, indicating that the salt undergoes a transition to an insulating state. An application of pressure enhances the metallic behavior.

The intermolecular overlap integrals among HOMOs of the donor molecules are listed in Table 5. Although we assumed that every ET molecule has the same formal charge in this calculation, the result is well informative as the first step to understand the electronic structure. The band structures of **1** and **2** are shown in Fig. 5. They have 10 branches and the eighth and ninth branches cross the Fermi level. These salts are considered as semimetals. Thanks to the Se atoms, the band width of **2** is larger than that of **1**, which should contribute to the enhanced metallic behavior of **2** together with the reduced on-site Coulomb repulsion. It should be noted that this system would have a cylindrical Fermi surface similar to that of the conventional θ-type salts if the formal charge of the donor molecule were $+\frac{1}{2}$ (corresponding to the $\frac{3}{4}$-filled band).

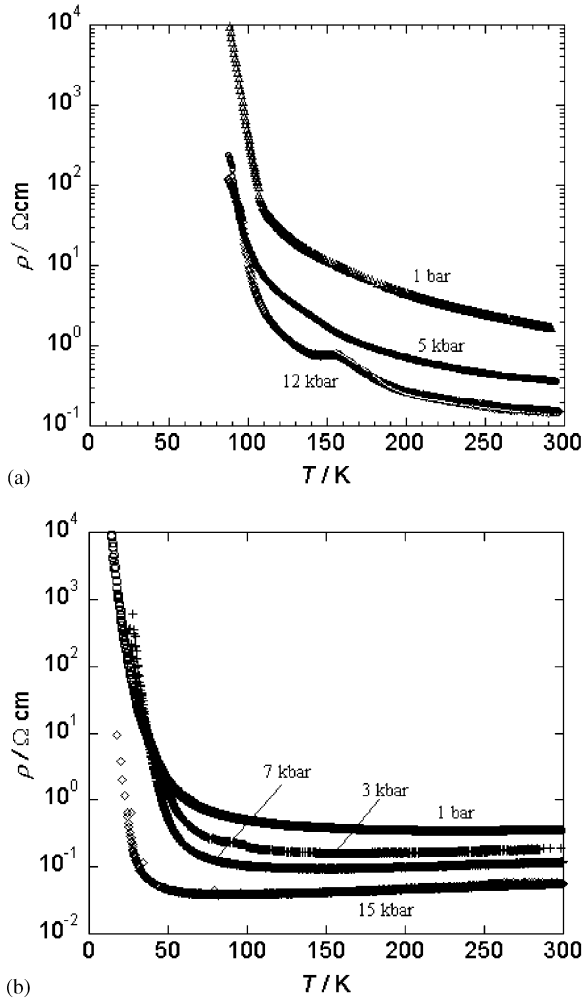

FIG. 4. Temperature dependence of resistivity for **1** (a) and **2** (b) under pressure.

*(ET)$_4$TeI$_4$ (**3**)*

A single crystal suitable for the X-ray structural analysis was obtained by galvanostatic electrolysis of a solution containing ET and $Bu^n_4N \cdot TeI_3$ in 1,2-dichloroethane or CH_2Cl_2. As shown in Fig. 6, the crystal structure of this salt is based on the herring-bone arrangement of ET molecules, similar to that of the α-type salt (14). The unit cell contains five crystallographically independent ET molecules. Two types of donor stacks (I and II) are observed. The stack I consists of weakly dimerized ET molecules (A and B). These dimerized molecules exhibit a zigzag stacking in accordance with the anion arrangement, which is not observed in the usual α-type donor arrangement. The stack II contains three crystallographically independent ET molecules (C, D, and E in Fig. 6), which are arranged in the sequence ···EDCD··· with a four-fold periodicity. The ET molecules are overlapped with a transverse shift parallel to the short molecular axis and with a longitudinal shift between the dimers in the stack I (Figs. 6c and 6d). This longitudinal shift seems to correspond to the thickness of the anion. Short S···S intermolecular contacts are observed between neighboring stacks but not within the stack (Table 6). The dihedral angles range from 131.8° to 134.7°. A bond lengths examination suggests that the formal charge of the donor molecules A and C is larger than that of the others (B, D and E), but it is difficult to determine the exact value due to less accuracy of the crystal structure analysis.

The TeI_4^{2-} anions are located between donor layers. Only one slightly short I···I distance (3.92 Å) is observed between neighboring anions and there is no distinguishable anion network structure. No short I···H distance is found between the donor and the anion.

The room-temperature resistivity of **3** at ambient pressure ($\rho_{r.t.}$) is 0.5 Ω cm. The salt **3** is a semiconductor with relatively large activation energy ($E_a = 0.15$ eV, Fig. 7). A transition to an insulating state is observed at 210 K. The temperature dependence of the resistivity (in the ***ac*** plane) under pressure shows a quite unique behavior (Fig. 7). In the low-pressure region (< 3.5 kbar), the transition temperature increases up to about 230 K with increasing pressure. Further pressurization, however, lowers the transition temperature, and a metallic region appears around room temperature above 12 kbar.

The intermolecular overlap integrals among HOMOs of the donor molecules are listed in Table 7. In contrast to the case of the conventional α-type salts, the transverse interactions (*p* and *q*) are smaller than those along the stacking direction (*a* and *b*). The electronic band structure of **3** was calculated under the tight-binding approximation. The calculated electronic band structure and Fermi surface are shown in Fig. 8. There are eight branches and the sixth and the seventh branches cross the Fermi level, indicating a semimetallic character. The Fermi surface consists of two-dimensional pockets.

*(EDT-TTF)$_4$TeI$_4$ (**4**)*

A single crystal suitable for the X-ray structural analysis was obtained by galvanostatic electrolysis of a solution containing EDT-TTF and $Bu^n_4N \cdot TeI_3$ in CH_2Cl_2 at 5°C. As shown in Fig. 9, **4** has a layered structure of EDT-TTF molecules. The unit cell contains 16 donor molecules, all of which are crystallographically equivalent. The head-to-tail EDT-TTF dimers are arranged in a head-to-head fashion along the ***c***-axis and with a transverse shift along the ***b***-axis. Within the conduction layer, one dimer is surrounded by six neighboring dimers. Short S···S intermolecular contacts are observed along the ***b***-axis (side-by-side direction) but not along the ***c***-axis. This is a very unique two-dimensional donor arrangement which does not include the conventional column structure. The κ-type arrangement that is

TABLE 5
Calculated Overlap Integrals (S) among HOMOs ($\times 10^3$) for $(ET)_5Te_2I_6$ (1) and $(BETS)_5Te_2I_6$ (2)

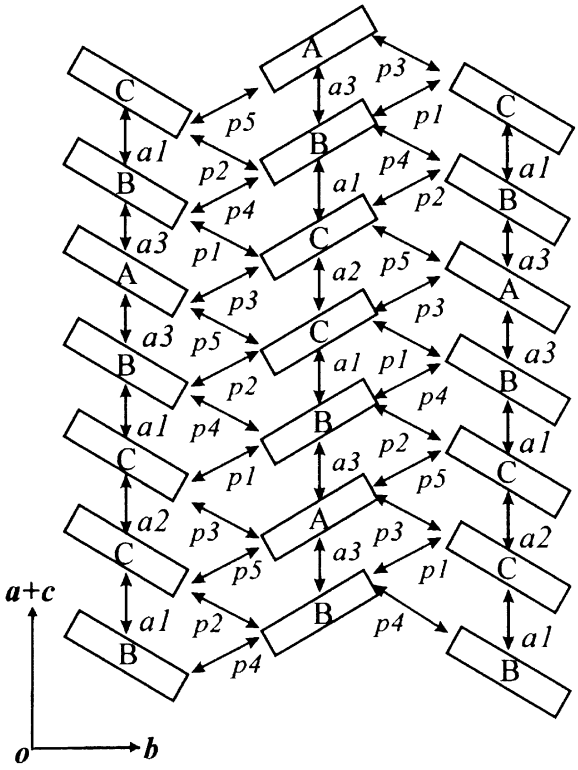

S	$(ET)_5Te_2I_6$ (**1**)	$(BETS)_5Te_2I_6$ (**2**)
$a1$	−3.66	−17.46
$a2$	0.14	−7.88
$a3$	−2.61	−15.25
$p1$	−2.37	−8.90
$p2$	−0.85	−4.72
$p3$	−2.18	−7.12
$p4$	−2.59	−7.88
$p5$	−1.51	−5.14

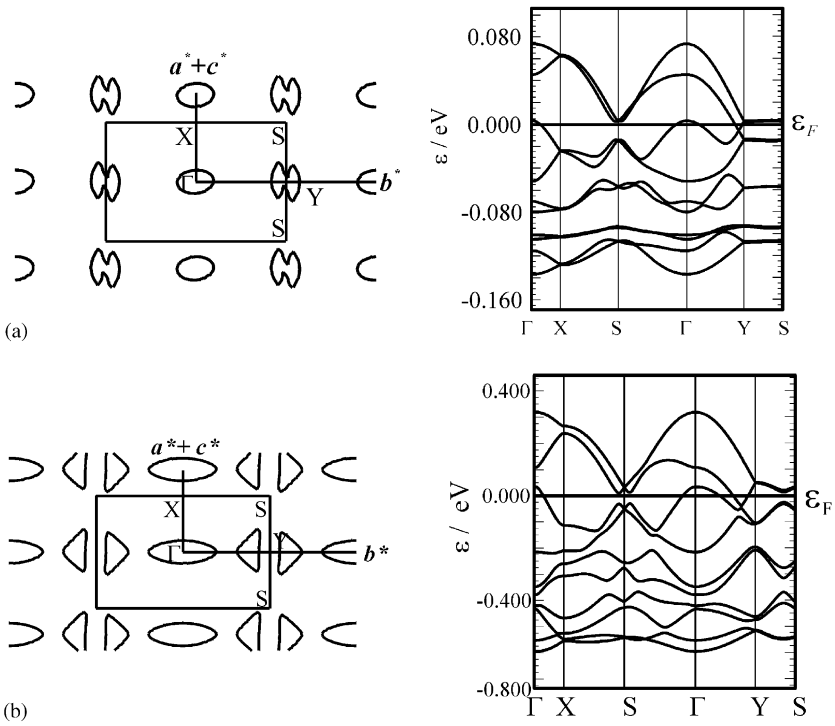

FIG. 5. Calculated band structures and Fermi surfaces for **1** (a) and **2** (b).

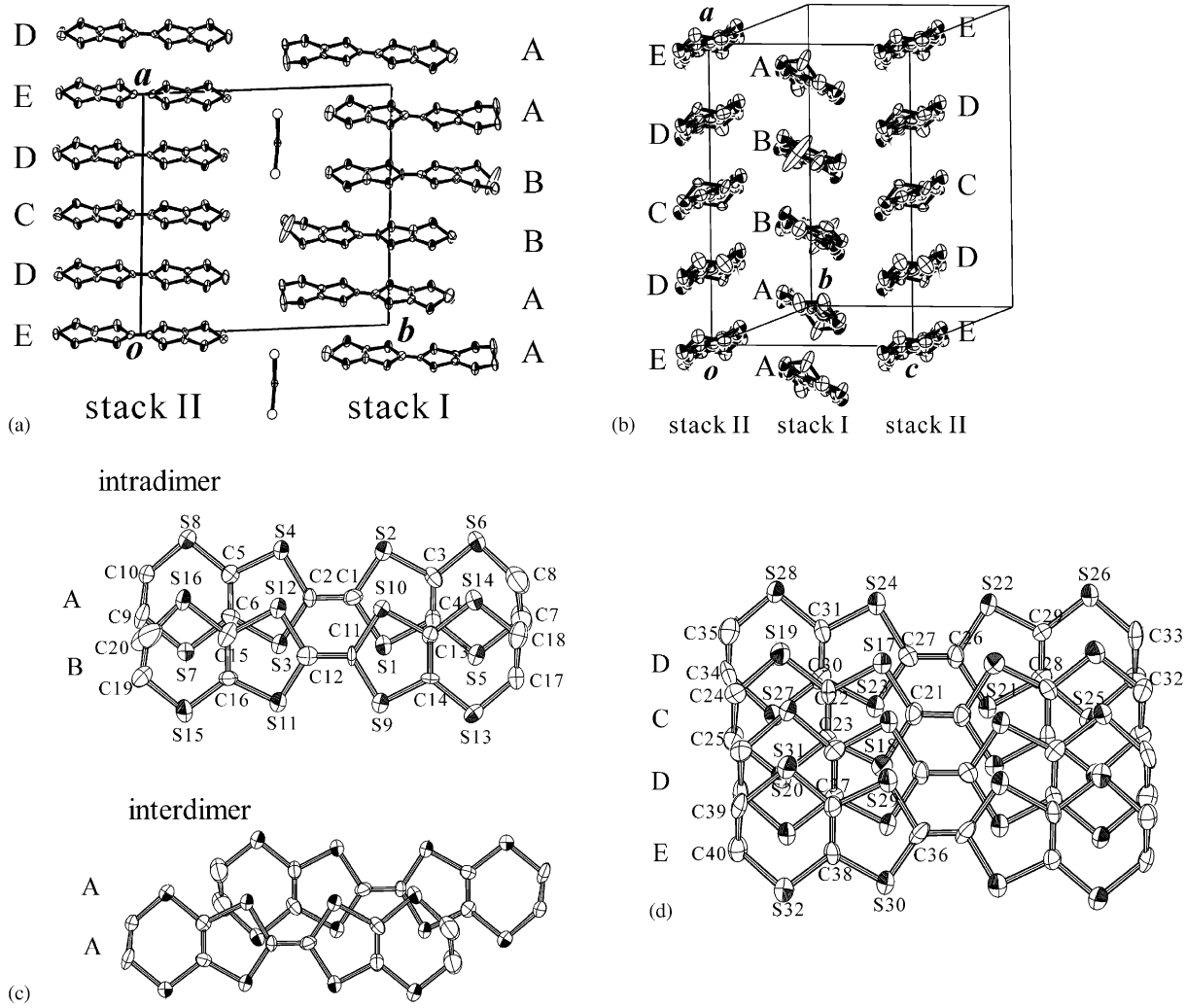

FIG. 6. Crystal structure of **3**: (a) viewed along the *c*-axis; (b) end-on projection of ET molecules; (c) overlap mode in stack I; (d) overlap mode in stack II.

TABLE 6
Short S ⋯ S Intermolecular Contacts in $(ET)_4TeI_4$ (3)

Atom	Atom	Distance	Atom	Atom	Distance
S(4)	S(25[a])	3.452(8)	S(12)	S(19[a])	3.558(8)
S(5)	S(31[b])	3.539(8)	S(13)	S(19[e])	3.479(8)
S(6)	S(32[c])	3.495(8)	S(14)	S(20)	3.491(8)
S(6)	S(30[c])	3.595(9)	S(14)	S(27[a])	3.594(8)
S(7)	S(26[d])	3.576(8)	S(14)	S(23[a])	3.595(8)
S(8)	S(25[a])	3.546(9)	S(15)	S(26[d])	3.533(8)
S(11)	S(26[d])	3.525(8)	S(16)	S(19[a])	3.502(8)

[a] $1-x, -y, -z$.
[b] $1+x, y, 1+z$.
[c] $1+x, y, z$.
[d] $1-x, -y, 1-z$.
[e] $x, y, 1+z$.

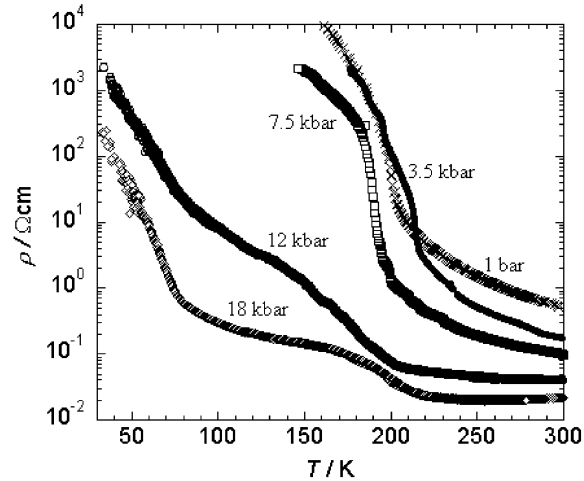

FIG. 7. Temperature dependence of resistivity for **3** under pressure.

TABLE 7
Calculated Overlap Integrals (S) among HOMOs ($\times 10^3$) for $(ET)_4TeI_4$ (3)

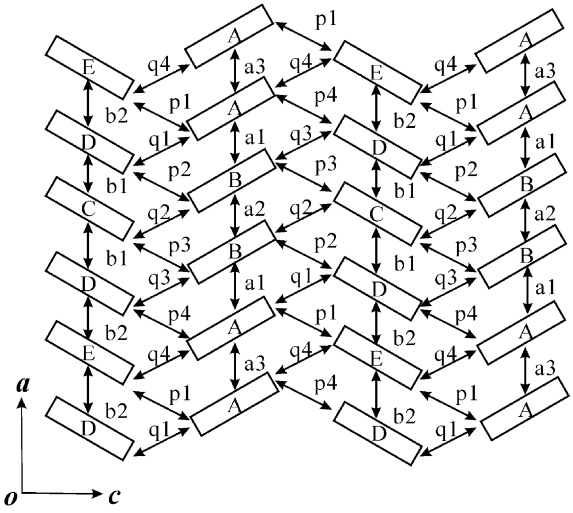

S	$(ET)_4TeI_4$(**3**)
$a1$	−4.98
$a2$	−1.09
$a3$	−1.40
$b1$	−2.69
$b2$	−7.47
$p1$	−1.76
$p2$	−1.72
$p3$	−1.70
$p4$	2.32
$q1$	−1.53
$q2$	−2.63
$q3$	−1.40
$q4$	−1.49

also based on the dimer contains the orthogonal packing of dimers. On the other hand, all the molecular planes are parallel to each other in the crystal of **4**. The anions fit into the caves on the donor layer. There is no short I···I distance between anions.

4 is a semiconductor with a room-temperature resistivity $\rho_{r.t.} = 20\,\Omega\,cm$ and an activation energy $E_a = 0.15\,eV$. With increasing pressure (up to 12 kbar), the $\rho_{r.t.}$ value decreases monotonically (down to $7\,\Omega\,cm$ at 12 kbar) but the E_a value is almost independent on the pressure. The calculated band structure of **4** is shown in Fig. 10. Inter-dimer interactions are rather two-dimensional within the conduction layer (Fig. 9). In this molecular packing, it is possible for an inter-layer interaction (s in Fig. 9) to exist, but its absolute value is still very small. There are eight branches and the eighth, ninth and tenth branches cross the Fermi level to afford a hole pocket around the Γ point and electron pockets around the V′ point. An origin of the semiconductive behavior even at room temperature is an open question.

*$(TMTTF)_2TeI_4$ (**5**) and $(HMTSF)_2Te_2I_6$ (**6**)*

The crystal of **5** is an insulator and formed by an alternating arrangement of the dimerized TMTTF unit and the TeI_4^{2-} anion along the ***b***-axis (Fig. 11). The TMTTF dimmers are stacked along the ***c***-axis. The resistivity of **5** at

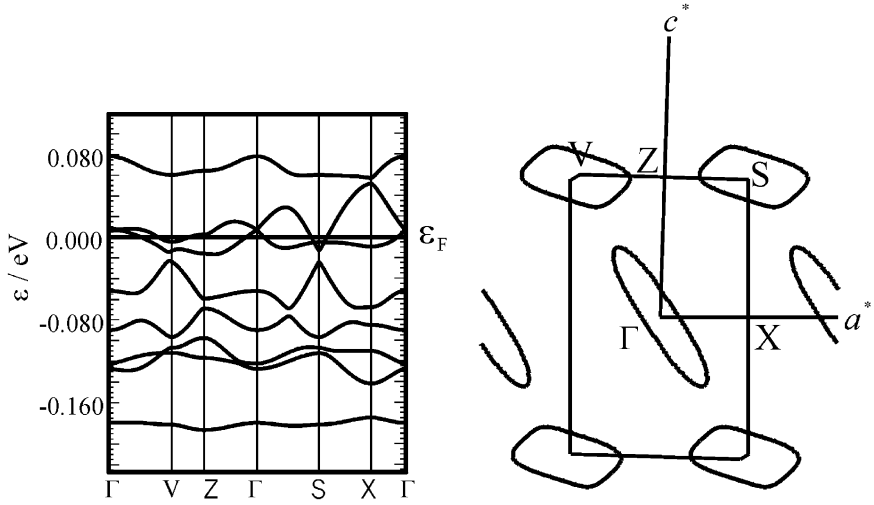

FIG. 8. Calculated band structure and Fermi surface for **3**.

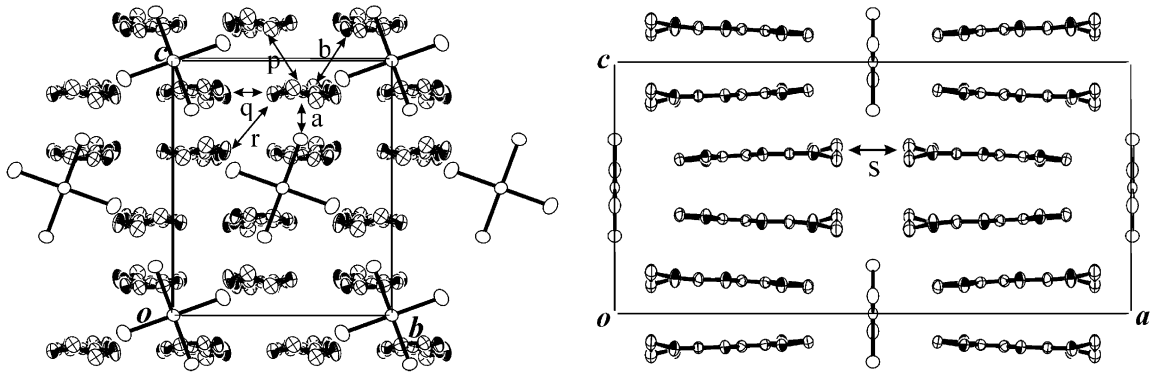

FIG. 9. Crystal structure of **4**: end-on projection (left) and side view (right). Overlap integrals among HOMOs ($\times 10^3$) are *a*, −14.99; *b*, −4.20; *p*, −0.90; *q*, 3.95; *r*, −6.21; *s*, 0.01.

room temperature $\rho_{r.t.}$ is $6 \times 10^3\,\Omega$ cm and the activation energy E_a is 0.15 eV.

As shown in Fig. 12, the crystal of **6** consists of alternating arrangements of the HMTSF unit and the $Te_2I_6^{2-}$ anion along the transverse direction. The HMTSF dimers are stacked along the ***c***-axis. Intermolecular Se···I (3.63–3.78 Å) and Se···Te (3.91 Å) contacts shorter than the sum of van der Waals radii (Se···I (3.88 Å) and Se···Te (4.00 Å)) are observed between the cation and anion. On the contrary to **2** and **3**, no distinguishable anion network is observed.

For both salts, the formal charge of the donor molecules is +1 and the one-dimensional columns have the two-fold periodicity. Therefore, they are considered to be a band insulator.

CONCLUSION

Two novel classes of square-planar Te(II)-iodide anions prepared by the new method have provided six new cation radical salts. X-ray crystal structure analyses revealed a variety of donor arrangements. As for donor molecules used in this work, the ability to form two-dimensional architectures decreases in the order BETS > ET > EDT-TTF > HMTSF, TMTTF. The donor arrangements obtained in this work can be classified into three categories:

(1) The herring-bone arrangement with two-dimensional intermolecular interactions (α- or θ-type; **1**, **2**, and **3**).

(2) The two-dimensional arrangement of dimers with molecular planes parallel to each other (**4**).

(3) The one-dimensional column of dimers whose side-by-side interactions are interrupted by the anions (**5** and **6**).

Among them, the herring-bone arrangements that provide the semimetallic band structures are of special interest in relation with the ultra-narrow-gap semiconductor α-$(ET)_2I_3$. Recently, it has been reported that α-$(ET)_2I_3$ with temperature-independent resistivity has a very high carrier mobility (up to ca. $3 \times 10^5\,cm^2/V$) comparable to those of inorganic semiconductors such as GaAs (15). Further study on transport properties will need to be carried out to clarify the nature of conduction electrons in these salts.

The formal charge of the donor molecule ranges from $+\frac{2}{5}$ to +1. The $Te_2I_6^{2-}$ anion has ability to form

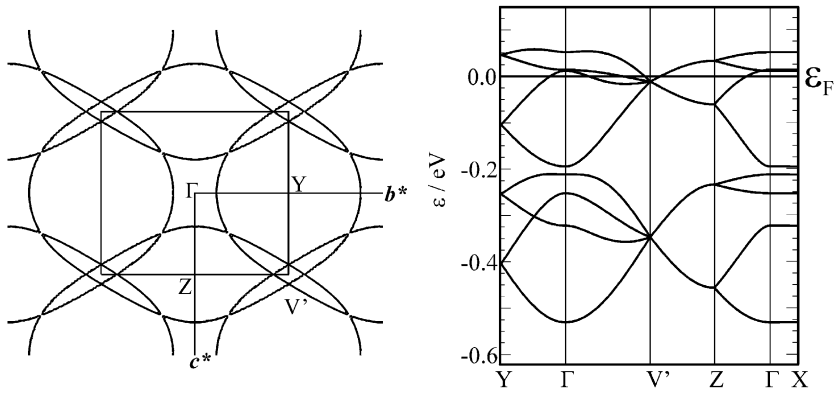

FIG. 10. Calculated band structure and Fermi surface for **4**.

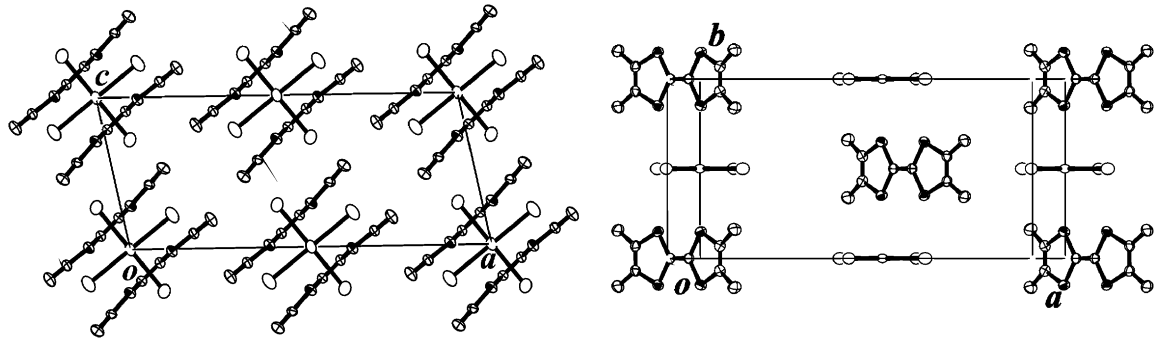

FIG. 11. Crystal structure of **5**: side view (left) and top view (right).

the new type of network assembly through intermolecular I···I contacts and suggests feasible control of the formal charge of the donor molecule by tuning the unit area of the anion network. The planar Te(II)-iodide anions will enable further salts to be obtained and thereby enhance our understanding of the role that the counteranions play in the conducting cation radical salts.

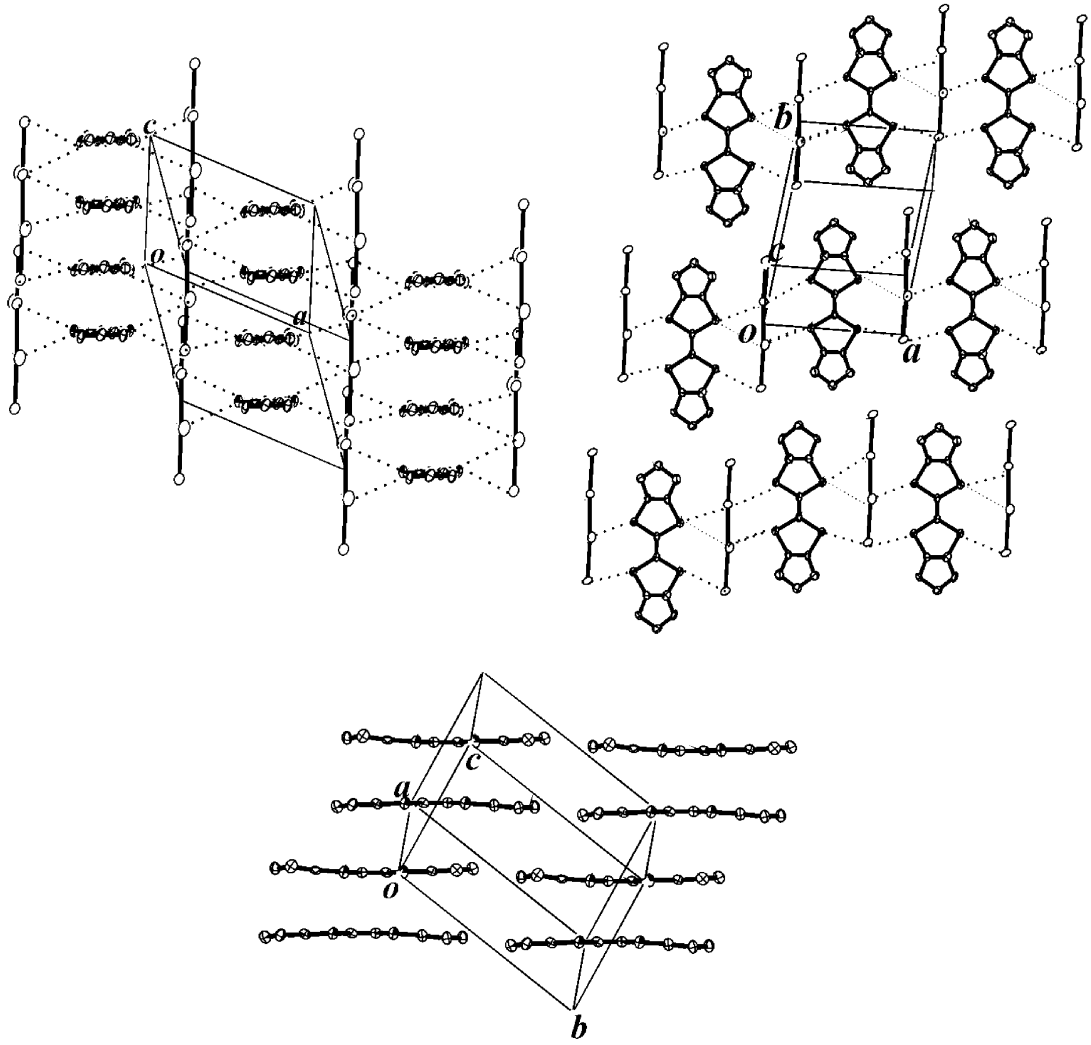

FIG. 12. Crystal structure of **6**: (a) top view; (b) end-on projection; (c) side view of HMTSF molecules.

ACKNOWLEDGMENT

This work was partially supported by a Grant-in-Aid for Scientific Research on Priority Areas (No. 10149103 ''Metal-assembled Complexes'') from Ministry of Education, Science, Sports and Culture, Japan.

REFERENCES

1. (a) T. Ishiguro, K. Yamaji, and G. Saito, ''Organic Superconductors,'' Springer-Verlag, Berlin, Heidelberg, 1998; (b) J. M. Williams, J. R. Ferraro, R. J. Thorn, K. D. Carlson, U. Geiser, H. H. Wang, A. M. Kini, and M.-H. Whangbo, ''Organic Superconductors (Including Fullerenes) Synthesis, Structure, Properties and Theory.'' Prentice-Hall, Englewood Cliffs, NJ, 1992.
2. (a) H. Urayama, H. Yamochi, G. Saito, K. Nozawa, T. Sugano, M. Kinoshita, S. Sato, K. Oshima, A. Kawamoto, and J. Tanaka, *Chem. Lett*. 55 (1988); (b) A. M. Kini, U. Geiser, H. H. Wang, K. D. Carlson, J. M. Williams, W. K. Kwok, K. G. Vandervoort, J. E. Thompson, D. L. Stupka, D. Jung, and M.-H. Whangbo, *Inorg. Chem*. **29,** 2555 (1990); (c) J. M. Williams, A. M. Kini, H. H. Wang, K. D. Carlson, U. Geiser, L. K. Montgomery, G. J. Pyrka, D. M. Watkins, J. M. Kommers, S. J. Boryschuk, A. V. Strieby Crouch, W. K. Kwok, J. E. Schirber, D. L. Overmyer, D. Jung, and M.-H. Whangbo, *Inorg. Chem*. **29,** 3262 (1990).
3. (a) H. Mori, S. Tanaka, T. Mori, and Y. Maruyama, *Bull. Chem. Soc. Jpn*. **68,** 1136 (1995); (b) H. Mori, S. Tanaka, T. Mori, A. Kobayashi, and H. Kobayashi, *Bull. Chem. Soc. Jpn*. **71,** 797 (1998); (c) P. Batail, K. Boubekeur, M. Fourmigué, and J.-C. P. Gabriel, *Chem. Mater*. **10,** 3005; (1998); (d) A. Deluzet, P. Batail, Y. Misaki, P. Auban-Senzier, and E. Canadell, *Adv. Mater*. **12,** 436 (2000).
4. (a) H. M. Yamamoto, J. Yamaura, and R. Kato, *J. Am. Chem. Soc*. **120,** 5905 (1998); (b) H. M. Yamamoto and R. Kato, *Chem. Lett*. 970 (2000).
5. B. Krebs and F.-P. Ahlers, *Adv. Inorg. Chem*. **35,** 235 (1990).
6. N. W. Alcock, *Adv. Inorg. Chem. Radiochem*. **15,** 1 (1972).
7. (a) HMTSF: Y. Okano, H. Sawa, S. Aonuma, and R. Kato, *Chem. Lett*. 1851 (1993). (b) EDT-TTF: R. Kato, H. Kobayashi, and A. Kobayashi, *Chem. Lett*. 781 (1989); (c) ET: K. S. Varma, A. Bury, N. J. Harris, and A. E. Underhill, *Synthesis* 837 (1987); (d) BETS: R. Kato, H. Kobayashi, and A. Kobayashi, *Synth. Met*. **42,** 2093 (1991).
8. M. E. Demarçay, *Bull. Soc. Chim*. **40,** 99 (1883).
9. R. Hoffman, *J. Phys. Chem*. **39,** 1397 (1963).
10. (a) T. Mori, A. Kobayashi, Y. Sasaki, H. Kobayashi, G. Saito, and H. Inokuchi, *Bull. Chem. Soc. Jpn*. **57,** 627 (1984); (b) M.-H. Whangbo, J. M. Williams, P.C. W. Leung, M. A. Beno, T. J. Emge, H. H. Wang, K. D. Carlson, and G. W. Crabtree, *J. Am. Chem. Soc*. **107,** 5815 (1985).
11. S. Pohl, W. Saak, and B. Krebs, *Z. Naturforsh*. **40b,** 251 (1985).
12. P. Guionneau, C. J. Kepert, G.Bravic, D.Chasseau, M. R. Truter, M. Kurmoo, and P. Day, *Synth. Met*. **86,** 1973 (1997).
13. (a) H. Kobayashi, H. Tomita, T. Naito, A. Kobayashi, F. Sakai, T. Watanabe, and P. Cassoux, *J. Am. Chem. Soc*. **118,** 368 (1996); (b) N. D. Kushch, O. A. Dyachenko, V. V. Gritsenko, P. Cassoux, C. Faulmann, A. Kobayashi, and H. Kobayashi, *J. Chem. Soc. Dalton Trans*. 683 (1998); (c) I. Malfant, T. Courcet, C. Faulmann, P. Cassoux, H. Gornitzka, F. Granier, M.-L. Doublet, P. Guionneau, J. A. K. Howard, N. D. Kushch, and A. Kobayashi, *C. R. Acad. Sci. Paris Série IIc* **4,** 149 (2001).
14. T. Mori, H. Mori, and S. Tanaka, *Bull. Chem. Soc. Jpn*. **72,** 179 (1999).
15. N. Tajima, M. Tamura, Y. Nishio, K. Kajita, and Y. Iye, *J. Phys. Soc. Jpn*. **69,** 543 (2000).